Vibrational Spectroscopy of Crystalline Multilayer Ice: Surface Modes in the Intermolecular-Vibration Region

T. Yamada, H. Okuyama,* T. Aruga, and M. Nishijima

Department of Chemistry, Graduate School of Science, Kyoto University, Kyoto 606-8502, Japan

Received: June 20, 2003; In Final Form: September 8, 2003

Vibrational studies have been made of single-crystalline ice by the use of electron energy loss spectroscopy (EELS). The EELS spectra exhibit vibrational features due to the surface as well as the bulk molecules. To differentiate between the surface and bulk modes, we examine primary energy dependence of the spectra and the adsorption of additional water molecules on the "clean" ice surface to selectively perturb the surface vibrations. Surface optical modes are detected in the intermolecular vibrational-energy region, and we observe a loss at 100 (95) cm^{-1} which is ascribed to the hindered-translational vibration of the outermost H_2O (D_2O) along the surface normal direction. The surface hindered-rotational modes are observed at 470, 665, and 825 (355, 500, and 620) cm^{-1}. We suggest that the water molecules initially adsorbed on the ice surface are isolated and not clustered at 85 K. The admolecules are metastable at 85 K and restructure to form a stable bilayer-terminated ice surface at 128 K.

1. Introduction

As one of the most common materials in nature, solid ice has been studied in various fields such as environmental sciences and astrophysics.[1] Ozone depletion involves chlorine activation on ice clouds in the polar stratosphere; hence, much effort has been devoted to the study of chemical reactions on the ice surface, where the activation is believed to occur.[2,3] To understand the reaction mechanisms on ice, it is essential to study the fundamental properties of the ice surface. The crystalline ice surface has been a subject of many researchers, and a great deal of work has focused on its dynamical properties such as surface diffusion[4] and surface melting.[5] Despite an increasing interest in the ice surface, vibrational properties of the ice surface are not well understood, especially in the intermolecular vibrational region.

Vibrational studies of the crystalline bulk ice have been performed by means of infrared reflection absorption spectroscopy (IRAS),[6−9] Raman spectroscopy,[9,10] and inelastic neutron scattering.[11] A great deal of data have been accumulated to date covering the entire energy region of vibrations, providing us with fruitful information on the physical properties of bulk ice. On the other hand, vibrational investigations of the ice surface have been restricted to a few studies, probably due to the sensitivity problem of the experimental techniques. By the use of IRAS, Devlin et al.[12] observed the O−H stretch modes of water at the polycrystalline ice surface. Combined with molecular dynamics calculations, they ascribed several vibrational features to the water molecules at the surface or subsurface of the ice. More recent He-atom scattering study reported by Glebov et al.[13] succeeded in detecting surface acoustic phonons (Rayleigh modes) for the first time.

Crystalline ice thin film is known to be grown on the (111) surfaces of face-centered-cubic metals or (0001) surfaces of hexagonal-close-packed metals under ultrahigh vacuum.[14,15] By means of dynamical low-energy electron diffraction (LEED) combined with total energy calculations, Materer et al.[16] revealed the layered stacking structure of crystalline ice thin film grown on Pt(111) substrate, and found that the ice film on a Pt(111) is the common hexagonal I_h with the (0001) basal plane exposed to the vacuum. The total energy calculations suggest that the full-bilayer termination is energetically more favorable than the half-bilayer termination at the surface and the outermost layer has lower vibrational frequency than in the bulk due to its reduced hydrogen bonding-coordination. Wei et al.[5] applied sum-frequency generation to probe the surface structure of the ice thin film. They found that the outermost-layer disordering, i.e., the surface melting occurs at 200 K.

In our previous study,[17] we reported the observations of the surface optical modes of ice in the energy region 30−300 cm^{-1} (hindered-translational vibration region). It was shown that high-resolution electron energy loss spectroscopy (EELS) has sufficient sensitivity to the surface vibrations of crystalline ice thin films. Compared to the other vibrational spectroscopy techniques mentioned above, the advantages of EELS with its wide spectral range and high surface sensitivity are obvious. In this paper, we report the observations of the surface optical modes of crystalline ice in the whole range of the vibrations. We succeed in the resolutions of several surface-derived modes from the bulk modes. In the intermolecular-vibration region, we observe losses at 100, 470, 665, and 825 cm^{-1} for H_2O ice. The isotope-labeled experiments clearly assign the 100 cm^{-1} mode as a hindered translation and the others as hindered rotations. The EELS intensities of these modes are sensitive to the adsorption of additional water molecules, which indicates that these modes are derived from the surface. We investigate the electron scattering mechanism from the ice, and find that the surface modes are excited via the dipole mechanism in contrast to the bulk modes which show a characteristic resonance feature.

2. Experimental Section

All experiments were performed using an ultrahigh vacuum (UHV) chamber equipped with a high-resolution electron energy loss spectrometer (LK-5000, LK Technologies, Inc.), a four-

* Corresponding author. E-mail: hokuyama@kuchem.kyoto-u.ac.jp.

10.1021/jp035753x CCC: $25.00
Published on Web 11/19/2003

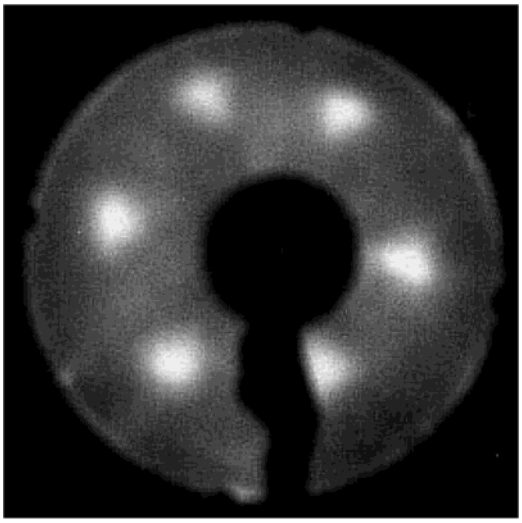

Figure 1. A LEED pattern from the crystalline ice thin film (10 BL, D_2O) deposited on Pd(111) taken with $E_p = 44$ eV and the sample current ~40 nA. The pattern was obtained in ~5 min, after the electron beam was switched on, to reduce the beam-induced effect. The (1×1) spots indicate the single-crystalline ice with the (0001) plane of the I_h phase exposed to the vacuum. The large spot size and high background intensity are ascribed to the large vibrational amplitudes of the surface water molecules.

grid retarding-field analyzer for LEED ,and a quadrupole mass spectrometer for thermal desorption measurements.

A Pd(111) sample was cleaned by cycles of Ar ion sputtering (500 eV) and annealing (1100 K), followed by the oxidation and reduction cycles. The cleanness of the sample was checked by LEED and EELS, which suggested no trace of impurity. The crystalline ice thin film was prepared by exposing the clean Pd(111) surface to gaseous H_2O or D_2O via a tube doser positioned ~15 mm apart from the surface. To ensure the crystallization of ice, the first bilayer was prepared at the rate of 0.1 BL/min at the substrate temperature of 148 K, followed by the multilayer deposition at 128 K at the rate of 0.5 BL/min (1 BL = 1 bilayer = 1.02×10^{15} water molecules/cm^2). The amount of ice was determined with thermal desorption spectroscopy.[18] The film thickness used in this study was 10 BL. After the preparation of crystalline ice thin film, the sample was cooled to 85 K, where EELS measurements were conducted. The background pressure was maintained below 6×10^{-11} Torr, and thus, the adsorption of the residual gases (mainly water) on the ice surface was negligible.

In this work, the crystalline ice thin film showed a 6-fold symmetric (1×1) LEED pattern as shown in Figure 1, which was similar to the case of crystalline ice multilayers grown on the Pt(111) substrate.[16] Thus, we consider that the ice I_h forms on Pd(111) mainly with the (0001) plane exposed to the vacuum. The (1×1) LEED pattern from ice thin film is characterized by the relatively larger spots with higher background intensity as compared to that from clean Pd(111), which indicates larger vibrational amplitude of water molecules in the outermost surface layer.[16]

All EELS spectra were recorded with the electron incidence (θ_i) and reflection (θ_r) angles with respect to the surface normal of 60° (specular mode). It is noted that all the surface modes observed in this study were found to be excited by the dipole mechanism from the angular dependent measurements.[19] It is known that low-energy electrons irradiated on the ice induce the dissociation of water molecules with the threshold energy estimated to be 10 eV.[20] Thus, we used the primary electron energy E_p below 8 eV and the sample current of 20−30 pA.

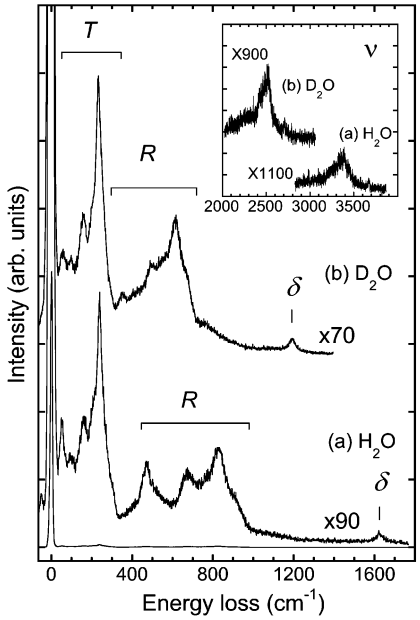

Figure 2. Typical EELS spectra of 10 BL crystalline ice thin films for (a) H_2O and (b) D_2O in the specular mode, $\theta_i = \theta_r = 60°$. $E_p = 2.8$ eV. The notations *T*, *R*, and δ indicate the modes due to hindered-translations, hindered-rotations and scissors, respectively. In the inset, the O−H(O−D) stretch vibration (ν) is shown.

During the prolonged measurements (1 h), the elastic as well as inelastic peak intensities were unchanged, which indicates negligible damage of ice due to the electron beam irradiation of EELS. Typical energy resolution was 12−16 cm^{-1}.

3. Results and Discussion

Figure 2(a) and 2(b) show typical EELS spectra for H_2O and D_2O 10 BL crystalline ice in the range of 30−4000 cm^{-1}, respectively. The notations *T*, *R*, δ, and ν (inset) represent the modes of hindered translations, hindered rotations, scissors, and O−H(O−D) stretches, respectively, as assigned from the observed isotope energy ratios and the known values for gaseous water.[21] In the following, we discuss the vibrational spectra for the *T*, *R*, and ν modes separately.

3.1. Hindered Translations. *3.1.1. Detection of Surface Vibrational Modes.* The spectra (a) in Figure 3(A) and 3(B) are taken for 10 BL H_2O and D_2O ice, where five losses are observed (labeled as T_1-T_5), respectively. The E_p is 2.8 eV, and the intensities of the loss spectra are normalized to those for the elastic peaks. The observed losses are presented in Table 1. The T_3, T_4, and T_5 modes were observed in previous infrared studies for the bulk crystalline ice I_h,[8] indicating that these three modes are ascribed to the bulk. Taking the factor group to be isomorphous with D_{6h}, the strongest T_5 mode was assigned as the zone-center vibrations of the symmetry species A_{1g} and E_{1g}, or the zone-center vibration of the symmetry species E_{2g}. The T_3 and T_4 modes were assigned as the zone-center vibrations of the symmetry species B_{1g} and B_{2u}, respectively. These vibrations are dipole (infrared) active because the hydrogen atoms in ice crystals are not in the center of the O−O bonds. Besides, the broad features of the bulk modes are ascribed to the irregular orientations of water molecules in the ice I_h, where all the vibrations (not only the zone-center modes) are dipole active. It is noted that only the zone-center vibrations are allowed for the orientationally ordered regular crystals, where the vibrational spectra are characterized by the sharp peaks as observed for ice II and ice IX.[7]

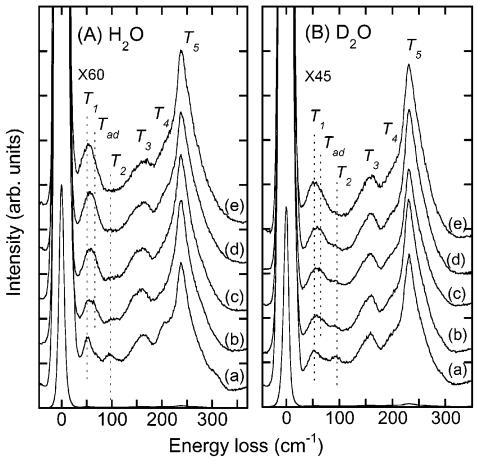

Figure 3. EELS spectra in the hindered-translational vibration region of 10 BL crystalline (A) H_2O and (B) D_2O, on which various amounts of H_2O and D_2O are adsorbed at 85 K, respectively. The amounts of adsorbed water are (a) 0, (b) 0.1, (c) 0.2, (d) 0.4, and (e) 0.7 BL. E_p = 2.8 eV. The T_2 mode is attenuated after the adsorption, indicating that this mode is derived from the surface, whereas the higher-energy losses T_3-T_5 due to the bulk water are relatively unaffected. A shoulder (denoted by T_{ad}) appears after the adsorption.

TABLE 1: Summary of the Observed Losses (in cm^{-1}) Whose Origins Are Represented by S, B, and AD Indicating Surface, Bulk, and Adsorption, Respectively

mode	H_2O	D_2O	ω_H/ω_D	origin
T_1	50	50	1.00	S
T_2	100	95	1.05	S
T_3	165	160	1.03	B
T_4	~200	~190	~1.05	B
T_5	240	230	1.04	B
T_{ad}	~65	~60	~1.1	AD
R_1	470	355	1.32	S
R_2	665	500	1.33	S
R_3	825	620	1.33	S,B
R_4	~890	~670	~1.33	B
R_5	~1120	~830	~1.35	B
R_{ad}	400			AD
δ	1620	1195	1.36	
ν_1	2960	2220	1.33	
ν_2	~3100	~2320	~1.34	B
ν_3	3250	2430	1.34	B
ν_4	~3340	~2470	~1.35	B
ν_5	3390	2520	1.35	S
ν_6	3680	2710	1.36	S,AD
ν_{ad}	3000	2250	1.33	AD

On the other hand, T_1 and T_2 were not observed in the infrared studies.[8] The spectra (b)−(e) in Figure 3(A) and 3(B) show the variations of the EELS spectra of 10 BL crystalline H_2O and D_2O, on which small amounts of additional H_2O and D_2O molecules are adsorbed at 85 K, respectively. The amount of the adsorbed water are (b) 0.1, (c) 0.2, (d) 0.4, and (e) 0.7 BL. In contrast to the T_3-T_5 modes whose intensities show little change, the T_2 mode is attenuated after the adsorption. The adsorption perturbs the outermost layer of ice selectively and quenches the surface modes, indicating that the T_2 mode is derived from the surface. An ab initio total energy calculation predicted the effective force constant of outermost water molecule along the surface normal direction to be 11.9 kcal (mol Å^2)$^{-1}$ which is about one-third of that obtained for the bulk ice.[16] Consequently, vibrational energies of the motion along this direction for H_2O (18 amu) and D_2O (20 amu) are roughly deduced to be 87 and 83 cm^{-1} within the harmonic approximation, respectively. The reduction of hydrogen-bonds at the surface (3-coordination) results in the lowering of the vibrational energy compared to that of bulk (4-coordination). Thus we assign the T_2 as the hindered-translational mode of the outermost $H_2O(D_2O)$ along the surface normal direction.

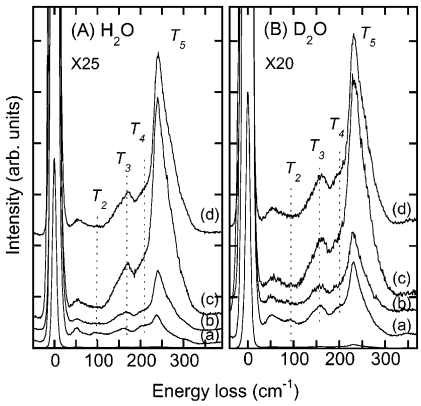

Figure 4. EELS spectra in the hindered-translational vibration region of 10 BL crystalline (A) H_2O and (B) D_2O as a function of E_p. The spectra are recorded at E_p of (a) 2.8, (b) 4.5, (c) 6.3, and (d) 7.8 eV. The intensities are normalized to those of the elastic peaks. The loss peaks show characteristic E_p dependences. With increasing E_p up to ~7 eV, the intensity of the surface mode T_2 decreases while those of the bulk modes T_3-T_5 are enhanced.

After the adsorption, we observe a new loss labeled as T_{ad} at ~65(60) cm^{-1} for $H_2O(D_2O)$, which appears as a shoulder of T_1. For the spectrum (b) in Figure 3(A), we decompose the ~50 cm^{-1} feature with Gaussian peaks and confirmed the contributions of two components at 50 cm^{-1} (T_1) and ~65 cm^{-1} (T_{ad}). T_{ad} may be ascribed to the water adspecies on the ice surface, but it cannot be ruled out that the crystalline ice surface is perturbed by the adsorption and gives rise to the T_{ad} mode.

The T_2 mode is assigned as the hindered-translational mode of the 3-coordinated surface molecules. We tentatively ascribe the T_1 to the low-coordinated water molecules on the ice surface possibly present at the bilayer steps or domain boundaries; the peak intensity of the T_1 is not reproducible and depends on the preparation of the ice film. It is noted that, in the previous He-atom scattering study,[13] a vibrational mode similar to T_1 was observed on a crystalline H_2O at 44−48 cm^{-1} between 30 and 120 K, which was assigned as the frustrated vibrational mode of an isolated admolecular species.

3.1.2. E_p Dependence of the Spectra. Figure 4(A) shows EELS spectra of 10 BL H_2O ice as a function of E_p. The corresponding spectra for D_2O ice are shown in Figure 4(B). The E_p are (a) 2.8, (b) 4.5, (c) 6.3, and (d) 7.8 eV, and the intensities are normalized to those of the elastic peaks. The bulk modes, T_3 and T_5, are increased in intensity at higher E_p. On the other hand, the surface mode T_2 is clearly observed only at lower E_p. To understand the E_p dependence of the loss intensities, we examine the scattering mechanism of electrons from the ice surface. In Figure 5, we plot the peak intensities normalized to those of the elastic peaks ($I_{loss}/I_{elastic}$) for the T_5 and T_2 modes as a function of E_p. From the dipole theory of electron scattering from surfaces, the intensities of the loss peaks can be represented by[19]

$$I_{loss}/I_{elastic} = (\pi e^{*2}\cos^2\theta_d N_s/911\hbar\omega\mu E_p\cos\theta_i) \times F(\gamma,\theta_i) \quad (1)$$

where e^* is the dynamic effective charge, θ_d the angle of the dynamic dipole moment with respect to the surface normal, N_s the number of the adsorbed species per unit area, $\hbar\omega$ the vibrational energy, μ the reduced mass of the oscillator, and θ_i the angle of incident electrons with respect to the surface normal. μ is in atomic mass units and the others are in atomic units. e^*

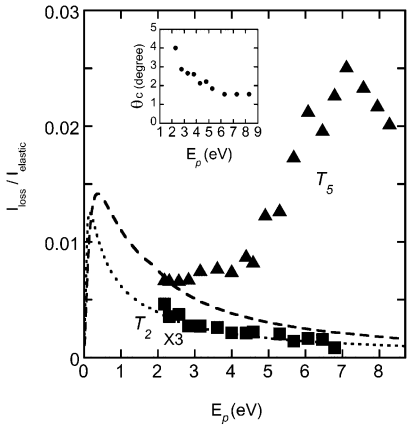

Figure 5. The intensities of the T_2 and T_5 modes normalized to those of the elastic peaks are shown as a function of E_p. The experimental results are given by filled squares and triangles, respectively. The dotted and dashed curves are calculated for T_2 and T_5 from the dipole theory, to fit the data points at 2.3 eV, respectively. The parameters used are $e^* = 0.17$ for T_2 and 0.35 for T_5 with θ_d assumed to be 0°. The inset shows the acceptance half angle of the spectrometer (θ_c) as a function of E_p, which is used for the calculations. Obviously, the maximum at ~7 eV of the experimental data for T_5 cannot be reproduced by the dipole theory.

and θ_d are unknown, and are used as parameters to fit the theoretical values to the experimental results. The angular term $F(\gamma,\theta_i)$ is given by

$$F(\gamma,\theta_i) = (\sin^2\theta_i - 2\cos^2\theta_i)/(1+\gamma^2) + (1+\cos^2\theta_i)\ln(1+1/\gamma^2) \quad (2)$$

and

$$\gamma = \theta_E/\theta_c,\ \theta_E = \hbar\omega/2E_p \quad (3)$$

where θ_c is the acceptance half-angle of the spectrometer and θ_E the beam parameter. θ_c is determined by the angle-dependent measurements of the elastic peak intensities, and the results are shown in the inset of Figure 5.

The calculated values for $I_{loss}/I_{elastic}$ are represented by the dotted curves in Figure 5. It is noted that the curves are calculated to fit the data point at $E_p = 2.3$ eV. Assuming that the dynamic dipole moment is normal to the surface ($\theta_d = 0°$), e^* is deduced to be 0.17 for T_2 and 0.35 for T_5 at $E_p = 2.3$ eV, respectively, and the estimated values of e^* seem reasonable.[22]

In Figure 5, the calculated values $I_{loss}/I_{elastic}$ for T_2 agree well with the experimental results. On the other hand, the E_p dependence of T_5 is obviously far from that predicted from the dipole theory. The intensity has a broad maximum around 7 eV, which indicates the contribution of the short-range resonance scattering mechanism. It is tentatively suggested that the negative ion "clusters" are temporarily formed by the trapping of the incident electrons and that the T_5 mode is excited during their decay process into the ground state. On the other hand, Michaud and Sanche[23] investigated the E_p dependence of EELS from amorphous ice at 14 K. It was found that the vibrational excitation cross section of the hindered-translational mode was enhanced at E_p ~7 eV, which was attributed to the resonance formation of the $^2B_1$ anion state. They proposed that the transient anion state decays via the long-range dipole interaction into the intermolecular modes of the surrounding molecules. It is noted that Michaud and Sanche,[23] in the analysis of their data, assumed a very low value of the dielectric constant ($\epsilon = 1.42$).

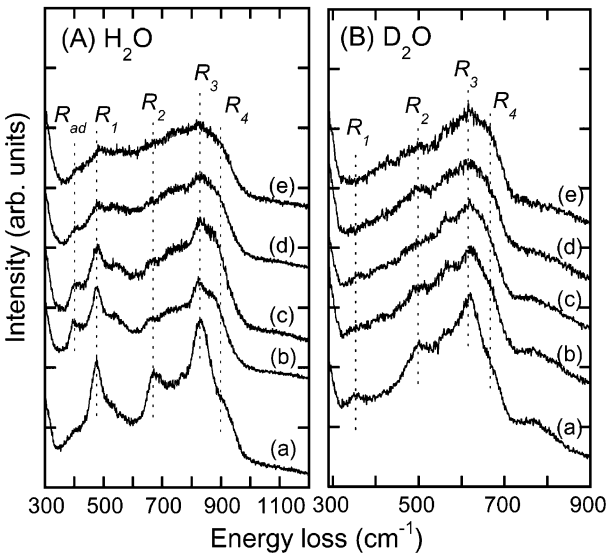

Figure 6. EELS spectra in the hindered-rotational vibration region of 10 BL crystalline (A) H_2O and (B) D_2O, on which various amounts of (A) H_2O and (B) D_2O are adsorbed at 85 K, respectively. The amounts of the adsorbed water are (a) 0, (b) 0.1, (c) 0.2, (d) 0.4, and (e) 0.7 BL. The intensities are normalized to those of the elastic peaks. $E_p = 2.8$ eV. The R_1, R_2, and R_3 modes are attenuated after the adsorption, indicating that these modes are derived from the surface (The R_3 mode has a contribution from the bulk, see text). A peak (denoted by R_{ad}) appears after the adsorption.

Finally, it is emphasized, strictly speaking, that eq 1 is applicable to surfaces of high dielectric constant ($\epsilon \gg 1$), and application to the ice ($\epsilon \sim 180$ at 130 K[24]) may be questionable.[19] Nevertheless, we believe the use of eq 1 is justified for qualitative arguments. To summarize, the resonance effect causes the characteristic E_p dependence of the bulk modes, which is absent for the surface modes. Thus we can use the E_p dependence of the individual peak intensities to differentiate the surface modes from the bulk modes of ice.

3.2. Hindered Rotations. *3.2.1. Detection of Surface Modes.* The losses in the region of 400−1200 (300−900 in D_2O) cm^{-1} are mainly assigned as the hindered-rotational modes. The spectra (a) in Figure 6(A) and 6(B) are taken for the 10 BL H_2O and D_2O ice, respectively ($E_p = 2.8$ eV). The intensities of the spectra are normalized to the elastic peak intensities. The variations of the spectra due to the adsorption of additional water molecules at 85 K are shown in (b)−(e). The amounts of the adsorbed water are (b) 0.1, (c) 0.2, (d) 0.4, and (e) 0.7 BL.

In the spectra of the clean ice for H_2O, three losses are distinctly observed at 470, 665, and 825 cm^{-1}, which are labeled as R_1, R_2, and R_3, respectively. At the higher-energy side of R_3, a shoulder is observed at ~890 cm^{-1} which is labeled as R_4. For D_2O, the losses are observed at 355, 500, 620, and ~670 cm^{-1} for R_1, R_2, R_3, and R_4, respectively. After the adsorption, the three main peaks R_1−R_3 are attenuated, indicating that they are derived from the surface. The adsorption of 0.4 BL water is enough to quench the surface modes, which is consistent with the case for the hindered translations. Note that the double-loss peak of the intense T_5 mode (see section 3.1.2) overlaps the R_1 for H_2O and R_2 for D_2O. The infrared study of the bulk ice in the rotational region showed a peak at 840 cm^{-1} with a shoulder at ~900 cm^{-1} for H_2O.[6] Thus, it is suggested that the bulk mode contributes to the R_3 peaks. The R_4 is the bulk mode. The observed losses are summarized in Table 1 except for the peak around 780 cm^{-1} resolved only in the spectra (a) of Figure 6(B). The origin of the 780 cm^{-1} peak is not well understood.

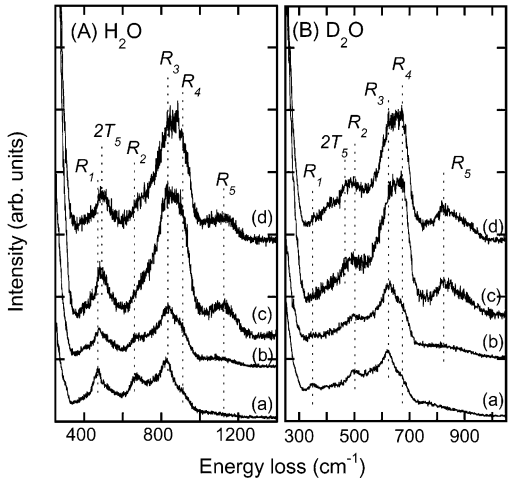

Figure 7. EELS spectra in the hindered-rotational vibration region of 10 BL crystalline (A) H_2O and (B) D_2O as a function of E_p. The spectra are recorded at E_p of (a) 2.8, (b) 4.5, (c) 6.3, and (d) 7.8 eV. The intensities are normalized to those of the elastic peaks. The surface modes R_1 and R_2 are well resolved only at lower E_p. Note that the double-loss peak of the intense T_5 mode (denoted by $2T_5$) for H_2O (D_2O) appears at 480 (460) cm^{-1} in the spectra (c) and (d). The surface R_3 mode is overlapped with the bulk mode which is enhanced at higher E_p. The R_4 mode is the bulk mode and enhanced at higher E_p.

Upon the adsorption of 0.1 BL H_2O [spectrum (b) in Figure 6(A)], a new peak is distinctly observed at 400 cm^{-1}, which is labeled as R_{ad}. The corresponding mode for D_2O cannot be resolved and may be buried in the intense tail of the T_5 mode. As in the case of the hindered translation T_{ad}, this peak is ascribed either to the adspecies or to the water molecules of crystalline ice modified by the water adsorption.

3.2.2. E_p Dependence of the Spectra. Figure 7(A) and 7(B) show the E_p dependences of the EELS spectra for H_2O and D_2O in the hindered-rotational region, respectively. The E_p are (a) 2.8, (b) 4.5, (c) 6.3, and (d) 7.8 eV. The R_1 and R_2 are clearly observed only at low E_p, supporting the assignments of these two losses as the surface modes. At high E_p [spectra (c) and (d)], the double-loss peak of the T_5 mode is observed at 480 (460) cm^{-1} (labeled as $2T_5$). The intensity ratios $I_{elastic}/I_{T5}$ and I_{T5}/I_{2T5} are similar, which supports the assignment of the double-loss peak. The R_4 mode is relatively intense in (c), which is ascribed to the resonance effect characteristic of the bulk modes. The R_3 mode appears to be enhanced in (c), but this is perhaps due to the overlap with the bulk mode. At higher E_p [(c) and (d)], the R_5 mode appears at ~1120 and 830 cm^{-1} for H_2O and D_2O, respectively. We assign the R_5 mode to the hindered rotation of the bulk, although the corresponding vibrational mode has not been observed in the past studies.

3.3. O−H(O−D) Stretch Modes. The spectra (a) in Figure 8(A) and 8(B) are taken for the clean ice surface of H_2O and D_2O in the O−H(O−D) stretch vibrational region, respectively (E_p = 2.8 eV). We observe the main loss at 3390(2520) cm^{-1} for $H_2O(D_2O)$, which is labeled as ν_5. A shoulder ν_3 is observed at the lower-energy side of ν_5. The spectrum (a) exhibits a sharp peak ν_6 at 3680(2710) cm^{-1} associated with the stretch vibration of free O−H(O−D) at the surface as described below.

The spectra (b) and (c) in Figure 8(A) and 8(B) are taken after the adsorption of additional water on the clean ice surface. To clarify the effect of the adsorption, we use the isotopes: Figure 8(A)[8(B)] show the variation of the spectra of $H_2O[D_2O]$ ice, on which $D_2O[H_2O]$ molecules are adsorbed. The amounts of the adsorbed water are (b) 0.4 and (c) 0.7 BL. In these experiments, the stretch modes of the adsorbed water are out

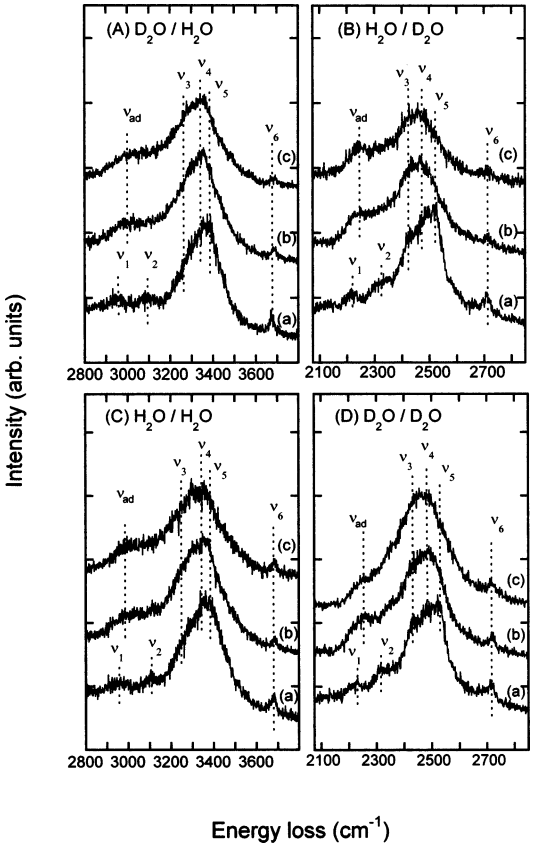

Figure 8. EELS spectra in the O−H(O−D) stretch vibrational region of the 10 BL crystalline ice, on which small amounts of water molecules are adsorbed at 85 K. E_p = 2.8 eV. The spectra are taken for various combinations of the isotopes: (A) D_2O on H_2O, (B) H_2O on D_2O, (C) H_2O on H_2O, and (D) D_2O on D_2O. The amounts of adsorbed water are (a) 0, (b) 0.4, and (c) 0.7 BL. The ν_5 and ν_6 modes in (A) and (B) are quenched by the adsorption, indicating that these are the surface modes. [The ν_6 modes in (C) and (D) have the contribution from the admolecules.]

of the spectral range. Thus, we can distinguish the peaks of adspecies and the crystalline surface (which is not possible in the intermolecular-vibration regime because of the smaller H_2O/D_2O isotope shifts). After the adsorption, the ν_5 and ν_6 decrease in intensity, which indicates that these two are the surface modes. On the other hand, the ν_3 and ν_4 modes show relatively small change and can be ascribed to the bulk. It is noted that clear distinction of the ν_4 and ν_5 modes can be made by the E_p-dependent measurements (Figure 9). At the clean ice surface, 3-coordinated water molecules exist with either free O−H (or dangling-H) or dangling-O coordination.[12] The ν_6 mode is due to the free O−H (dangling-H) species, while the ν_5 mode can be ascribed to the dangling-O species or 4-coordinated water molecules near the surface distorted with respect to the tetrahedral symmetry.[12] The observed modes are summarized in Table 1.

Figure 8(C)[8(D)] shows the variation of the spectra of $H_2O[D_2O]$ ice on which additional $H_2O[D_2O]$ molecules are adsorbed. In these spectra, the losses due to the adsorbed water are involved. Compared to Figure 8(A) and 8(B), the ν_6 mode appears to be unchanged due to the adsorption. This result can be interpreted as follows. The adsorbed water molecules quench the free O−H bonds at the ice surface, while they provide their free O−H bonds toward the vacuum. Thus the adsorbed water is not fully hydrogen-bonded at the surface. A loss is observed at the same energy of ~3000 cm^{-1} (labeled as ν_{ad}) after the adsorption of D_2O on H_2O [Figure 8(A)] or H_2O on H_2O [Figure

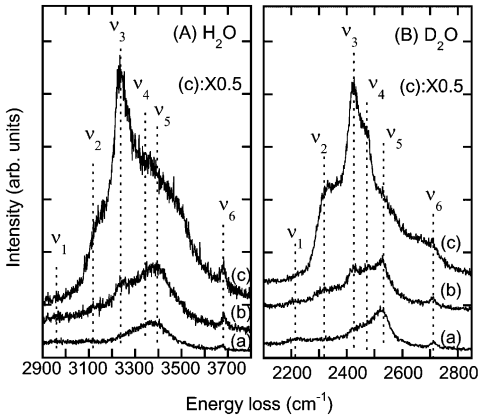

Figure 9. EELS spectra in the O−H(O−D) stretch vibrational region of 10 BL crystalline (A) H_2O and (B) D_2O as a function of E_p. The spectra are recorded at E_p of (a) 2.8 (b) 4.5, and (c) 6.3 eV. At higher E_p, the intensities of the bulk modes $\nu_2-\nu_4$ increase.

8(C)]. Thus the ν_{ad} peak is not ascribed to the adsorbed water itself but to the water molecules which belong to the crystalline ice prior to the water adsorption. It was proposed that the adsorption induces structural relaxation of the outermost layer due to the strained hydrogen-bondings.[25] The origin of the ν_{ad} mode may be related to the O−H stretch of the relaxed ice layer. The ν_2 mode is ascribed to the bulk ice as described in the next paragraph. The origin of the lowest-energy mode ν_1 is not known yet.

Figure 9(A) and 9(B) show the E_p dependences of the spectra for clean ice of H_2O and D_2O, respectively. The E_p are (a) 2.8, (b) 4.5, and (c) 6.3 eV. The intensities are normalized to those of the elastic peaks. The intensities of ν_5 and ν_6 are less sensitive to E_p, which supports the assignment of these peaks to surface modes. On the other hand, the intensities of $\nu_2-\nu_4$ are enhanced at $E_p = 6.3$ eV [spectra (c)], suggesting that these modes are derived from the bulk. In the infrared study of bulk ice, the O−H stretch modes were observed at 3150, 3220, and 3380 cm^{-1},[9] which is in agreement with our results. It is noted that a shoulder around 3500 cm^{-1} is observed at higher E_p only for H_2O ice [(c) in Figure 9(A)], but its origin is not well understood.

3.4. Water Adspecies on the Ice Surface. A recent theoretical study by Batista and Jónsson[25] predicts the existence of metastable water admolecules on the ice surface. Figure 10 shows the schematic models of water molecules adsorbed on the ice I_h surface. Due to the proton disorder, there are different kinds of adsorption sites on the surface. The admolecule forms hydrogen bondings with three or two water molecules in the first layer of ice. Adsorption sites are classified by the number of protons in the first layer pointing up toward the vacuum; the molecule (*a*) adsorbs on the site with one proton pointing up from the first layer, while the molecule (*b*) adsorbs on the site with two protons pointing up. The molecule (*b*) offers a free O−H bond toward the vacuum. The binding energies of these two species were calculated to be comparable (0.55−0.62 eV).[25] The molecule (*c*) with none of the three neighboring surface molecules has a proton pointing up from the first layer is less stable due to the reduced hydrogen-bonding. Note that the adsorption site with three protons pointing up is energetically unfavorable.[25] The diffusion barriers of the admolecules (*a*) and (*b*) on the ice surface were calculated to be 0.16−0.28 eV, which corresponds to the hopping rate at 85 K of the order 10^2-10^{-5} s^{-1}, assuming the prefactor of 10^{12} s^{-1}. Thus the admolecules may diffuse on the surface to form a cluster at 85 K. Indeed, a small cluster was proposed to form upon the adsorption of water

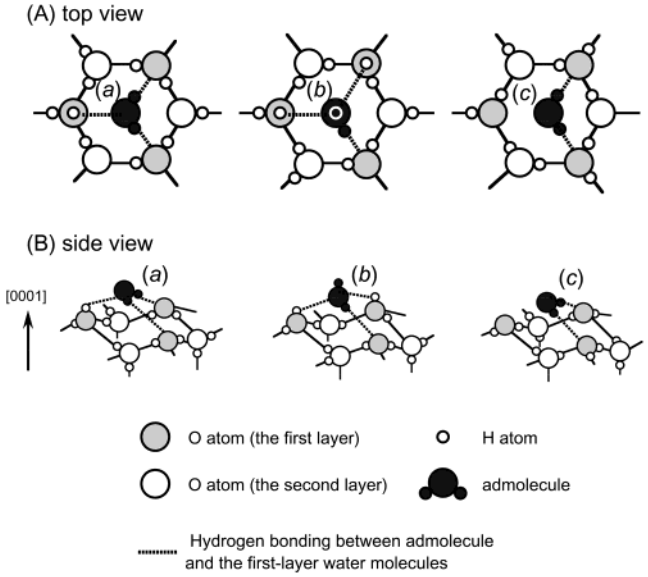

Figure 10. Structural models of the adsorbed water molecule on the (0001) surface of crystalline ice I_h: (A) top view, and (B) side view (ref 25). The admolecule forms hydrogen bondings to the water molecules in the first layer. Three kinds of configurations are shown which are denoted by (*a*), (*b*) and (*c*). Among these, the three-coordinated admolecules (*a*) and (*b*) were predicted to have comparable binding energies while the two-coordinated admolecule (*c*) less stable. Our results support the configuration (*b*) with a free O−H bond.

molecules on the ice surface even at 35 K.[26] In our experiments at 85 K, the quenching of the surface modes are complete after the adsorption of only 0.4 BL water molecules, which rules out the local formation of ice clusters on the ice surface. Thus, we suggest that the water molecules initially adsorbed on the ice surface at 85 K exist as isolated admolecules. As shown in Figure 8, it is found that the adsorbed water provides its free O−H bond, suggesting that the configuration (*b*) is supported from our experiments. It is noted that this does not exclude the existence of the configurations (*a*) and (*c*).

The adsorbed water is thermally metastable. Upon annealing the surface up to 128 K, the losses due to the adsorption (T_{ad}, R_{ad}, and ν_{ad}) disappear and the typical spectra of crystalline ice (Figure 2) are recovered. The desorption of water molecules from the ice film is known to occur above 130 K,[18] and thus, this result indicates that adspecies diffuse on the surface to form a more stable bilayer-terminated structure at 128 K. Although the growth mechanism of crystalline ice is complex and includes the formation of a variety of intermediates, such as dimer, trimer, and hexamer,[25] we propose that the metastable adspecies detected in this study play a key role as intermediates in the growth process of crystalline ice.

4. Conclusion

Surface vibrational modes for single-crystalline ice thin film have been studied by means of EELS. Surface modes are differentiated from the bulk modes by the primary electron energy-dependent measurements and water exposure-dependent measurements. We detect the surface modes in the intermolecular-vibrational region. We observe a loss at 100 (95) cm^{-1} for H_2O (D_2O) ice which is assigned as the hindered-translational mode of the outermost layer vibrating along the surface normal. In the hindered-rotational region, we observe surface modes at 470, 665, and 825 (355, 500, and 620) cm^{-1}. The surface phase O−H(O−D) stretch modes are observed at 3390 and 3680 (2520 and 2710) cm^{-1}. The EELS excitation mechanism for the surface

modes is found to be quite different from that for the bulk modes. The surface modes are mainly excited via the dipole mechanism, whereas the bulk modes show resonance features characteristic of the short-range mechanism. We suggest that the water molecules initially adsorbed on the ice surface are isolated and not clustered at 85 K. The admolecules are the intermediates in the growth process of ice, and they are metastable at 85 K and restructure to form a stable bilayer-terminated ice surface at 128 K.

Acknowledgment. Financial support for the present work was provided in part by the Grant-in-Aid for Scientific Research on Priority Areas "Surface Chemistry of Condensed Molecules" from the Ministry of Education, Culture, Sports, Science and Technology (Japan).

References and Notes

(1) Petrenko, V. F.; Whitworth, R. W. *Physics of Ice*; Oxford Unversity Press: New York, 1999.
(2) Roberts, J. T. *Acc. Chem. Res.* **1998**, *31*, 415.
(3) Girardet, C.; Toubin, C. *Surf. Sci. Rep.* **2001**, *44*, 159.
(4) Brown, D. E.; George, S. M. *J. Phys. Chem.* **1996**, *100*, 15460.
(5) Wei, X.; Miranda, P. B.; Shen, Y. R. *Phys. Rev. Lett.* **2001**, *86*, 1554.
(6) Bertie, J. E.; Whalley, E. *J. Chem. Phys.* **1964**, *40*, 1637.
(7) Bertie, J. E.; Labbé, H. J.; Whalley, E. *J. Chem. Phys.* **1968**, *49*, 775.
(8) Bertie, J. E.; Labbé, H. J.; Whalley, E. *J. Chem. Phys.* **1969**, *50*, 4501.
(9) Whalley, E. *Can. J. Chem.* **1977**, *55*, 3429.
(10) Wong, P. T. T.; Whalley, E. *J. Chem. Phys.* **1975**, *62*, 2418.
(11) Li, J. *J. Chem. Phys.* **1996**, *105*, 6733.
(12) Devlin, J. P.; Buch, V. *J. Phys. Chem. B* **1997**, *101*, 6095.
(13) Glebov, A.; Graham, A. P.; Menzel, A.; Toennies, J. P.; Senet, P. *J. Chem. Phys.* **2000**, *112*, 11011.
(14) Doering, D. L.; Madey, T. E. *Surf. Sci.* **1982**, *123*, 305.
(15) Thiel, P. A.; Madey, T. E. *Surf. Sci. Rep.* **1987**, *7*, 211.
(16) Materer, N.; Starke, U.; Barbieri, A.; Van Hove, M. A.; Somorjai, G. A.; Kroes, G. -J.; Minot, C. *Surf. Sci.* **1996**, *381*, 190.
(17) Okuyama, H.; Yamada, T.; Thachepan, S.; Aruga, T.; Nishijima, M. *Surf. Sci.* **2002**, *515*, L499.
(18) Wolf, M.; Nettesheim, S.; White, J. M.; Hasselbrink, E.; Ertl, G. *J. Chem. Phys.* **1991**, *94*, 4609.
(19) Ibach, H.; Mills, D. L. *Electron Energy Loss Spectroscopy and Surface Vibrations*; Academic Press: New York, 1982.
(20) Orlando, T. M.; Sieger, M. T. *Surf. Sci.* **2003**, *528*, 1.
(21) Eisenberg, D.; Kauzmann, W. *The Structure and Properties of Water*; Oxford University Press: New York, 1966.
(22) Ibach, H. *Surf. Sci.* **1977**, *66*, 56.
(23) Michaud, M.; Sanche, L. *Phys. Rev. Lett.* **1987**, *59*, 645.
(24) Johari, G. P.; Whalley, E. *J. Chem. Phys.* **1981**, *75*, 1333.
(25) Batista, E. R.; Jónsson, H. *Comput. Mater. Sci.* **2001**, *20*, 325.
(26) Pelmenschikov, A.; Ogasawara, H. *J. Phys. Chem. A* **2002**, *106*, 1695.